

## Gastight Hydrodynamic Electrochemistry: Design for a Hermetically Sealed Rotating Disk Electrode Cell

Suho Jung, Ruud Kortlever, Ryan J.R. Jones, Michael F Lichterman, Theodor Agapie, Charles C. L. McCrory, and Jonas C. Peters

*Anal. Chem.*, **Just Accepted Manuscript** • DOI: 10.1021/acs.analchem.6b04228 • Publication Date (Web): 07 Dec 2016

Downloaded from <http://pubs.acs.org> on December 9, 2016

### Just Accepted

“Just Accepted” manuscripts have been peer-reviewed and accepted for publication. They are posted online prior to technical editing, formatting for publication and author proofing. The American Chemical Society provides “Just Accepted” as a free service to the research community to expedite the dissemination of scientific material as soon as possible after acceptance. “Just Accepted” manuscripts appear in full in PDF format accompanied by an HTML abstract. “Just Accepted” manuscripts have been fully peer reviewed, but should not be considered the official version of record. They are accessible to all readers and citable by the Digital Object Identifier (DOI®). “Just Accepted” is an optional service offered to authors. Therefore, the “Just Accepted” Web site may not include all articles that will be published in the journal. After a manuscript is technically edited and formatted, it will be removed from the “Just Accepted” Web site and published as an ASAP article. Note that technical editing may introduce minor changes to the manuscript text and/or graphics which could affect content, and all legal disclaimers and ethical guidelines that apply to the journal pertain. ACS cannot be held responsible for errors or consequences arising from the use of information contained in these “Just Accepted” manuscripts.

# Gastight Hydrodynamic Electrochemistry: Design for a Hermetically Sealed Rotating Disk Electrode Cell

Suho Jung,<sup>†\*</sup> Ruud Kortlever,<sup>†</sup> Ryan J. R. Jones,<sup>†</sup> Michael F. Lichterman,<sup>†</sup> Theodor Agapie,<sup>†</sup> Charles C. L. McCrory,<sup>‡\*</sup> and Jonas C. Peters<sup>†\*</sup>

<sup>†</sup>Joint Center for Artificial Photosynthesis, California Institute of Technology, Pasadena, CA, 91125, United States

<sup>‡</sup>Department of Chemistry, University of Michigan, Ann Arbor, MI, 48104, United States

**Corresponding Author\*** suho.jung@gmail.com, cmccrory@umich.edu, jonas.peters@gmail.com

**ABSTRACT:** Rotating disk electrodes (RDEs) are widely used in electrochemical characterization to analyze the mechanisms of various electrocatalytic reactions. RDE experiments often make use of or require collection and quantification of gaseous products. The combination of rotating parts and gaseous analytes makes the design of RDE cells that allow for headspace analysis challenging due to gas leaks at the interface of the cell body and the rotator. In this manuscript we describe a new, hermetically-sealed electrochemical cell that allows for electrode rotation while simultaneously providing a gastight environment. Electrode rotation in this new cell design is controlled by magnetically coupling the working electrode to a rotating magnetic driver. Calibration of the RDE using a tachometer shows that the rotation speed of the electrode is the same as that of the magnetic driver. To validate the performance of this cell for hydrodynamic measurements, limiting currents from the reduction of a potassium ferrocyanide ( $K_4[Fe(CN)_6] \cdot 3H_2O$ ) were measured and shown to compare favorably with calculated values from the Levich equation and with data obtained using more typical, non-gastight RDE cells. Faradaic efficiencies of ~95% were measured in the gas phase for oxygen evolution in alkaline media at an Inconel 625 alloy electrocatalyst during rotation at 1600 rpm. These data verify that a gastight environment is maintained even during rotation.

## INTRODUCTION

Rotating disk electrode (RDE) voltammetry is a common electroanalytical tool that allows for the specific control of mass transfer of species at an electrode surface. This, in turn, allows for the decoupling of mass transfer kinetics from electron-transfer kinetics and chemical kinetics in an electrochemical system. RDE voltammetry and related hydrodynamic electroanalytical techniques have been extensively used in probing the electrochemical kinetics of many reactions including the oxygen reduction reaction (ORR),<sup>1-5</sup> the hydrogen oxidation reaction,<sup>6-8</sup> electrodeposition reactions,<sup>9-11</sup> and the CO<sub>2</sub> reduction reaction (CO<sub>2</sub>RR)<sup>12,13</sup>. Rigorous determination of product distribution of the electrochemical process under hydrodynamic conditions is required for the employment of rotating disk electrode (RDE) voltammetry in the study of electrocatalytic small-molecule transformations with multiple possible gaseous products, such as CO, H<sub>2</sub>, and hydrocarbons in the case of aqueous CO<sub>2</sub>RR. This requirement highlights the need for a gastight RDE apparatus in which both electrocatalytic kinetics and product distribution can be measured simultaneously.

RDE cells have been employed for the study of processes involving gaseous products and have relied on gastight seals between the rotator and the cell.<sup>8,12-16</sup> Herein we present an alternative design for a gastight RDE cell. Instead of attempting to form a seal with a rotating shaft, our design uses magnetic coupling through the electrochemical cell wall to transfer the mechanical momentum of rotation from an exterior motor to the rotating shaft of the working electrode housed within the

cell. This design has allowed us to realize a rigorously gastight RDE cell. Detailed descriptions of cell design, construction, and rotator calibration are provided here. Moreover, calibration of the rotator and the gastight cell design have been validated by (i) measuring the electrochemical mass transport-limited kinetics of potassium ferrocyanide using rotating disk electrode voltammetry, and (ii) confirming near unity Faradaic efficiency for electrocatalytic O<sub>2</sub> evolution by an Inconel 625 under constant rotation.

## EXPERIMENTAL

### Materials

All materials were used as received. Potassium ferrocyanide ( $K_4[Fe(CN)_6] \cdot 3H_2O$ , ≥99.0% trace metals basis), sodium hydroxide (NaOH, BioUltra grade), potassium dihydrogen phosphate (KH<sub>2</sub>PO<sub>4</sub>, BioUltra, ≥99.5%), and potassium hydrogen phosphate (K<sub>2</sub>HPO<sub>4</sub>, BioUltra, ≥99.0%) were purchased from Sigma Aldrich. Potassium nitrate (KNO<sub>3</sub>, Baker analyzed A.C.S. Reagent, ≥99.0%) was purchased from J.T. Baker. Nitrogen (N<sub>2</sub>) was boil-off gas from a liquid nitrogen source. All water used was purified with a Thermo Scientific Barnstead Nanopure water purification system (18.2 MΩ•cm resistivity).

### Electrochemical Measurements

Electrochemical measurements were conducted with a Bio-Logic VMP3 multichannel potentiostat/galvanostat with a built-in EIS analyzer. The working electrodes were 5 mm diameter, 4 mm thick disk electrodes, either made from Inconel

625 or from glassy carbon with a geometric surface area of 0.196 cm<sup>2</sup>, mounted into a Pine Instrument Company E6-series ChangeDisk RDE assembly affixed to the rotating shaft in the hermetically sealed electrochemical cell. For all of the electrochemical measurements, Ag/AgCl/1.0 M KCl (Ag/AgCl, CH Instrument) was used as a reference electrode, and carbon rod (99.999%, Strem Chemicals) was used as an auxiliary electrode. All potentials are reported versus the Ag/AgCl electrode used in this study.

The working electrode disks were prepared as follows. A rod of Inconel 625 was purchased from McMaster Carr and machined into 5 mm diameter and 4 mm thick disks. Sigradur G grade glassy carbon disks, dimensions of 5 mm diameter and 4 mm as received, were purchased from HTW Hochtemperatur-Werkstoff GmbH. The glassy carbon disks were polished and cleaned prior to each experiment using a previously reported procedure. Briefly, the disks were first lapped with 600-grit SiC grinding paper (Carbimet 2 600/P1200, Buehler) and then sequentially polished with 9 μm, 6 μm, 3 μm, 1 μm, and 0.1 μm diameter particle-based diamond polishing slurries (MetaDi Supreme, Buehler) on a synthetic nap polishing pad (MD Flocc, Struers). This was followed by sequential sonication for 10 min each in pure water, methanol, 2-propanol, acetone, and again in pure water.<sup>17-19</sup>

For all electrochemical measurements, the working electrode chamber contained 90.0 mL of electrolyte and the auxiliary electrode chamber contained 30.0 mL of electrolyte. The total headspace volumes of the working electrode and auxiliary electrode chamber were 50.1 mL and 16.5 mL, respectively.

For the rotating disk calibration measurements, 5 mm glassy carbon disk was used as a working electrode. 0.01 M K<sub>4</sub>[Fe(CN)<sub>6</sub>]•3H<sub>2</sub>O as a redox agent and 0.1 M KNO<sub>3</sub> as a supporting electrolyte were prepared in pure water. The solution was bubbled with N<sub>2</sub> for 20 minutes, followed by blanketing N<sub>2</sub> during the RDEV. Solution uncompensated resistance was estimated with ZIR function in the Biologic SW (EC-Lab, v10.44) and internally compensated at 85%. RDEV measurements were conducted as a function of rotation speed from 100 rpm to 3000 rpm at 100 mV/s of scan rate. Following the same protocol stated above, the same set of measurements was conducted using a typical 2 chamber-H cell (non-gastight cell) as a comparison. The comparison measurements were conducted using a Pine Research Instrumentation E6-series ChangeDisk RDE assembly affixed directly to a Pine Research Instrumentation MSR rotator. The measurements using the gastight RDE cell and the conventional RDE assembly were repeated 3 times, and the reported results are averages with reported standard deviations.

For the Faradaic efficiency measurements, a NeoFox fluorescence O<sub>2</sub> sensor (Ocean Optics) with a Foxy patch was used to measure the oxygen partial pressure in the headspace. The 1/8-inch diameter probe is inserted into the headspace with a Swagelok fitting to prevent leaking. Before the measurements, a two-point calibration was performed using constant flow of the compressed house air (20.9% O<sub>2</sub>) and the compressed house N<sub>2</sub> (0% O<sub>2</sub>). After the calibration the main chamber was brought to complete N<sub>2</sub> saturation again by sparging the electrolyte solution with N<sub>2</sub> for an hour. The N<sub>2</sub> flow was stopped prior to the electrolysis, and the gastight setup was monitored at open circuit for (10-15 minutes). Chronopotentiometry of Inconel 625 working electrode in 1M NaOH was run at 10 mA (approximately 51 mA/cm<sup>2</sup> for the 5

mm diameter disk) for one hour, before again being placed at open circuit. The O<sub>2</sub> detection was continued in the headspace for 20 min, to allow equilibration between the solution and gas phase. This equilibrium value was employed in the calculation of the amount of O<sub>2</sub> produced. The amount of charge passed was 36 coulombs. The amount of O<sub>2</sub> produced was corrected using the Henry's Law constant (770 L atm/mol for oxygen in pure water and the standard condition).<sup>20</sup>

## RESULTS AND DISCUSSION

### Cell Construction

The hermetically sealed RDE cell consists of two separable components: a standard borosilicate H-cell ubiquitous in electrochemical measurements (Adam and Chittenden), and a custom PTFE stopper. The H-cell working electrode chamber is in ionic communication with the counter electrode chamber through a glass frit bridge. The custom PTFE stopper has two circumferential O-rings, which create a hermetic seal in the working electrode chamber of the H-cell through radial compression when inserted from the top. This PTFE stopper was designed to accept all of the working electrode components of a standard RDE with careful consideration given to maintaining the rotating shaft assembly in a hermetically sealed environment (Figure 1). Control of the rotating shaft in its sealed environment is achieved using cylindrical magnets oriented in a planar configuration; a magnet mechanically secured to a Pine Research Instrumentation MSR electrode rotator drive shaft couples to a follower magnet secured to the shaft located in the sealed chamber. Electrical and mechanical ingress to the sealed environment is achieved using a combination of Swagelok and custom O-ring fittings. These fittings allow access to the sealed electrochemical environment during operation in a variety of ways and can therefore be used for general analytical purposes, i.e. liquid sampling, headspace sampling, and reference electrode positioning. Spring loaded silver-carbon brushes (Pine Research Instrumentation) are used to maintain electrical contact with the sealed rotating shaft during operation. When fully assembled, the total volume of the working electrode chamber and counter electrode chamber are 140.1 mL and 46.5 mL, respectively.

### Rotating Speed RPM Calibration

A tachometer (Fisher Scientific) was used to calibrate the speeds of both the driver magnet and the follower magnet. A reflective copper tape (0.5 inch x 0.5 inch) was attached onto the rotating shaft, and the tachometer was fixed by a clamp for steady positioning. The responding speeds of the driver and follower shafts as measured by the tachometer were plotted against those reported by the Pine MSR rotator motor (Figure 2). The calibration results indicate that the driver and follower speeds match the speed controlled by the MSR motor, ensuring that rotation of the working electrode can be accurately controlled.

### Rotating Disk Electrode Voltammogram (RDEV) Validation

RDEV measurements were conducted to further validate the rotation speed calibration of the rotating disk apparatus. Here, a 5 mm glassy carbon disk was rotated at various scan rates in an aqueous electrolyte solution containing 10 mM

1  $\text{Fe}(\text{CN})_6^{4-}$ . RDEVs were collected as a function of the rotating  
 2 speed from 100 rpm to 3000 rpm (Figure 3(a)).  $\text{Fe}(\text{CN})_6^{4-}$  is  
 3 oxidized to  $\text{Fe}(\text{CN})_6^{3-}$ , and replenished at the electrode as controlled  
 4 by the rotating electrode. This results in a steady-state  
 5 current at any given rotation rate which reaches a limiting  
 6 plateau value at potentials positive of  $\sim 0.8$  V vs Ag/AgCl  
 7 where the mass-transport of  $\text{Fe}(\text{CN})_6^{4-}$  to the surface becomes  
 8 rate limiting.

9 The mass transport of  $\text{Fe}(\text{CN})_6^{4-}$  can be modeled by the  
 10 Levich equation,<sup>21</sup> where the limiting plateau current,  $i_L$  at a  
 11 given rotation rate is given by:

$$12 \quad i_L = 0.62nFAD^{2/3}\omega^{1/2}\nu^{-1/6}[\text{Fe}(\text{CN})_6^{4-}] \quad (1)$$

13 where  $n = 1$  is the number of electrons in the oxidation,  $F$  is  
 14 Faraday's constant,  $A = 0.196$  cm<sup>2</sup> is the surface area of the  
 15 electrode,  $D = 0.65 \times 10^{-5}$  cm<sup>2</sup> s<sup>-1</sup> is the diffusion coefficient of  
 16  $\text{Fe}(\text{CN})_6^{4-}$  ion in 0.1 M aqueous electrolyte,<sup>22,23</sup>  $\omega = 2\pi(\frac{\text{rpm}}{60})$   
 17 is the angular rotation rate of the electrode,  $\nu = 0.00992$  cm<sup>2</sup> s<sup>-1</sup>  
 18 is the kinematic viscosity of 0.1 M KNO<sub>3</sub>,<sup>24</sup> and  $[\text{K}_4\text{Fe}(\text{CN})_6]$   
 19 =  $10^{-4}$  mol cm<sup>-3</sup> is the concentration of the substrate in the so-  
 20 lution. A Levich plot of the experimental limiting plateau  
 21 currents measured in the gastight RDE cell at 0.8 V vs  
 22 Ag/AgCl as a function of the square root of the rotation rate as  
 23 displayed by the Pine controller is linear (Figure 3b). The  
 24 experimental values measured in the gastight RDE cell match  
 25 well with calculated values from the Levich equation. In addition,  
 26 the same set of experiments were conducted using a traditional  
 27 RDE configuration with direct, mechanical attachment  
 28 of the rotating shaft to the rotator motor without the use of  
 29 magnetic coupling. The values from the gastight RDE cell  
 30 match well with the values measured using the traditional  
 31 RDE configuration in these studies, as well as those reported  
 32 in previous studies (Figure 3b).<sup>21</sup>

### 33 Faradaic Efficiency (FE) Validation

34 To confirm that the hermetically-sealed rotating disk electrode  
 35 cell is indeed gastight, the Faradaic efficiency of a  
 36 known oxygen-evolving electrocatalyst, an Inconel 625 disk  
 37 electrode,<sup>25-27</sup> was measured. The catalyst was held at a constant  
 38 applied anodic current of 51 mA cm<sup>-2</sup> for 1 h while being  
 39 rotated at a constant 1600 rpm. The oxygen content in the  
 40 headspace was monitored using a fluorescence-based O<sub>2</sub> sensor.<sup>28,29</sup>  
 41 Fig. 4 shows the expected theoretical O<sub>2</sub> partial pressure  
 42 versus the measured O<sub>2</sub> partial pressure in the headspace.  
 43 The offset between the start of electrolysis and the observed  
 44 O<sub>2</sub> response is attributed to the time required for O<sub>2</sub> to saturate  
 45 the electrolyte and enter the headspace.<sup>30,31</sup> After the electrolysis  
 46 was stopped, the system was allowed to equilibrate and the  
 47 measured O<sub>2</sub> values were observed to plateau. The average  
 48 Faradaic efficiency from three measurements was 95.8%  $\pm$   
 49 3.6%. This result confirms that the hermetically-sealed rotating  
 50 disk electrode cell remained gastight during electrode rotation  
 51 on the timescale of the experiment (1 hour).

### 52 CONCLUSION

53 We have reported the design, construction, calibration  
 54 and validation of a hermetically-sealed rotating disk electrode  
 55 cell. Communication between the rotator and the rotating

shaft is made via magnetic coupling. This enables the construction  
 of a cell that remains gastight during electrode rotation, a common  
 technical challenge faced by chemists/electrochemists seeking to  
 perform RDE voltammetry and quantitative (gas) product analysis.  
 The rotation response between the rotator motor and rotating shaft  
 has been calibrated using a tachometer and validated by measuring  
 the rotation kinetics of K<sub>4</sub>Fe(CN)<sub>6</sub> reduction. Finally, the  
 gastight nature of the cell has been validated by measuring near  
 unity Faradaic efficiency for water oxidation by a known oxygen  
 evolution catalyst through headspace analysis while simultaneously  
 rotating the electrode at a constant 1600 rpm. This cell design  
 should facilitate mechanistic studies of multi-electron transformations  
 in which gaseous products are produced and their distribution is  
 dependent on the local concentrations of reactants and intermediates  
 at the electrode surface.

### 56 AUTHOR INFORMATION

#### 57 Corresponding Author

58 \* suho.jung@gmail.com, cmccrory@umich.edu,  
 59 jonas.peters@gmail.com

### 60 ACKNOWLEDGMENT

This material is based upon work performed by the Joint Center  
 for Artificial Photosynthesis, a DOE Energy Innovation Hub, supported  
 through the Office of Science of the U.S. Department of Energy  
 under Award Number DE-SC0004993.

### REFERENCES

- (1) Marković, N. M.; Schmidt, T. J.; Stamenković, V.; Ross, P. N. *Fuel Cells* **2001**, *1*, 105-116.
- (2) Gasteiger, H. A.; Kocha, S. S.; Sompalli, B.; Wagner, F. T. *Appl. Catal., B* **2005**, *56*, 9-35.
- (3) Bing, Y.; Liu, H.; Zhang, L.; Ghosh, D.; Zhang, J. *Chem. Soc. Rev.* **2010**, *39*, 2184-2202.
- (4) Garsany, Y.; Baturina, O. A.; Swider-Lyons, K. E.; Kocha, S. S. *Anal. Chem.* **2010**, *82*, 6321-6328.
- (5) Suntivich, J.; Gasteiger, H. A.; Yabuuchi, N.; Shao-Horn, Y. *J. Electrochem. Soc.* **2010**, *157*, B1263-B1268.
- (6) Shao, M. *J. Power Sources* **2011**, *196*, 2433-2444.
- (7) Schmidt, T. J.; Gasteiger, H. A.; Stäb, G. D.; Urban, P. M.; Kolb, D. M.; Behm, R. J. *J. Electrochem. Soc.* **1998**, *145*, 2354-2358.
- (8) Armstrong, F. A.; Belsey, N. A.; Cracknell, J. A.; Goldet, G.; Parkin, A.; Reisner, E.; Vincent, K. A.; Wait, A. F. *Chem. Soc. Rev.* **2009**, *38*, 36-51.
- (9) Clarke, C. J.; Browning, G. J.; Donne, S. W. *Electrochim. Acta* **2006**, *51*, 5773-5784.
- (10) Estrine, E. C.; Riemer, S.; Venkatasamy, V.; Stadler, B. J. H.; Tabakovic, I. *J. Electrochem. Soc.* **2014**, *161*, D687-D696.
- (11) Yoshida, T.; Komatsu, D.; Shimokawa, N.; Minoura, H. *Thin Solid Films* **2004**, *451-452*, 166-169.
- (12) Hall, A. S.; Yoon, Y.; Wuttig, A.; Surendranath, Y. *J. Am. Chem. Soc.* **2015**, *137*, 14834-14837.
- (13) Wuttig, A.; Yaguchi, M.; Motobayashi, K.; Osawa, M.; Surendranath, Y. *Proc. Natl. Acad. Sci.* **2016**, *113*, E4585-E4593.
- (14) Bradley, P. E.; Landolt, D. *J. Electrochem. Soc.* **1997**, *144*, L145-L148.
- (15) Goldet, G.; Wait, A. F.; Cracknell, J. A.; Vincent, K. A.; Ludwig, M.; Lenz, O.; Friedrich, B.; Armstrong, F. A. *J. Am. Chem. Soc.* **2008**, *130*, 11106-11113.
- (16) Baturina, O. A.; Lu, Q.; Padilla, M. A.; Xin, L.; Li, W.; Serov, A.; Artyushkova, K.; Atanassov, P.; Xu, F.; Epshteyn, A.; Brintlinger, T.; Schuette, M.; Collins, G. E. *ACS Catal.* **2014**, *4*, 3682-3695.
- (17) Jung, S.; McCrory, C. C. L.; Ferrer, I. M.; Peters, J. C.; Jaramillo, T. F. *J. Mater. Chem. A* **2016**, *4*, 3068-3076.
- (18) McCrory, C. C. L.; Jung, S.; Ferrer, I. M.; Chatman, S.; Peters, J. C.; Jaramillo, T. F. *J. Am. Chem. Soc.* **2015**, *137*, 4347-4357.

- 1  
2  
3  
4  
5  
6  
7  
8  
9  
10  
11  
12  
13  
14  
15  
16  
17  
18  
19  
20  
21  
22  
23  
24  
25  
26  
27  
28  
29  
30  
31  
32  
33  
34  
35  
36  
37  
38  
39  
40  
41  
42  
43  
44  
45  
46  
47  
48  
49  
50  
51  
52  
53  
54  
55  
56  
57  
58  
59  
60
- (19) McCrory, C. C. L.; Jung, S.; Peters, J. C.; Jaramillo, T. F. *J. Am. Chem. Soc.* **2013**, *135*, 16977-16987.
- (20) Sander, R. *Atmos. Chem. Phys.* **2015**, *15*, 4399-4981.
- (21) Town, J. L.; MacLaren, F.; Dewald, H. D. *J. Chem. Edu.* **1991**, *68*, 352.
- (22) Bard, A. J.; Faulkner, L. R. *Electrochemical Methods: Fundamentals and Applications, 2nd ed.*; John Wiley & Sons, Inc.: Hoboken, NJ, 2001.
- (23) Adams, R. N. *Electrochemistry at Solid Electrodes*; Marcel Dekker, Inc.: New York, 1969.
- (24) *CRC Handbook of Chemistry and Physics*, 66 ed.; CRC Press: Boca Raton, FL, 1985-1986.
- (25) Corrigan, D. A. *J. Electrochem. Soc.* **1987**, *134*, 377-384.
- (26) Jayalakshmi, M.; Kim, W.-Y.; Jung, K.-D.; Joo, O.-S. *Int. J. Electrochem. Sci.* **2008**, *3*, 908-917.
- (27) Li, X.; Walsh, F. C.; Pletcher, D. *Phys. Chem. Chem. Phys.* **2011**, *13*, 1162-1167.
- (28) Demas, J. N.; DeGraff, B. A.; Coleman, P. B. *Anal. Chem.* **1999**, *71*, 793A-800A.
- (29) Spurgeon, J. M.; Velazquez, J. M.; McDowell, M. T. *Phys. Chem. Chem. Phys.* **2014**, *16*, 3623-3631.
- (30) Surendranath, Y.; Dincă, M.; Nocera, D. G. *J. Am. Chem. Soc.* **2009**, *131*, 2615-2620.
- (31) Dincă, M.; Surendranath, Y.; Nocera, D. G. *Proc. Natl. Acad. Sci.* **2010**, *107*, 10337-10341.

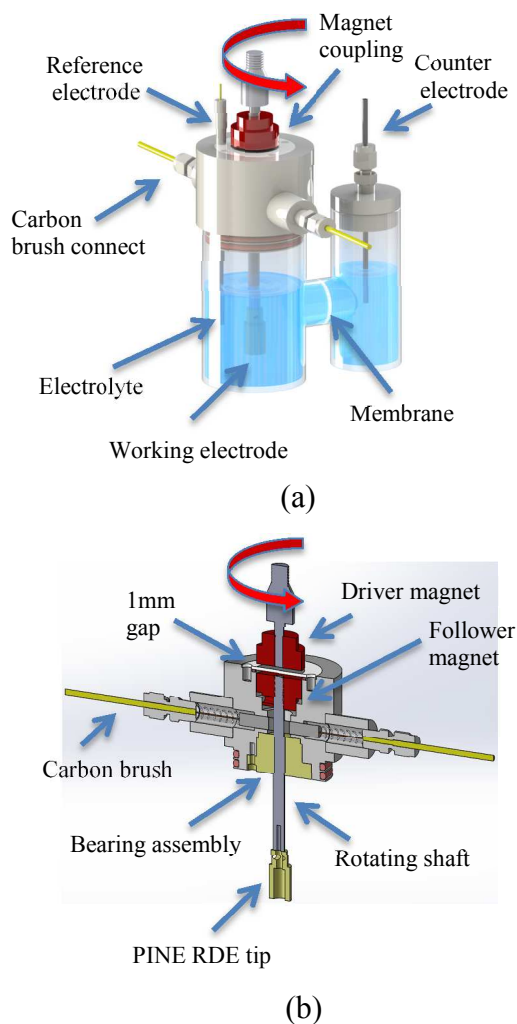


**Figure 1.** Schematics of the gastight RDE cell design. (a) The assembled two-chamber electrochemical cell separated by frit or membrane. The working electrode (5-mm dia. disk) chamber contained 90.0 mL of electrolyte and the auxiliary electrode chamber contained 30.0 mL of electrolyte. The total head-space volumes of the working electrode and auxiliary electrode chamber were 50.1 mL and 16.5 mL, respectively (b) The cross-section of the main chamber PTFE top, modified to fit various components such as follower magnet, a pair of carbon brush, a rotating stainless steel shaft, and a bearing assembly.

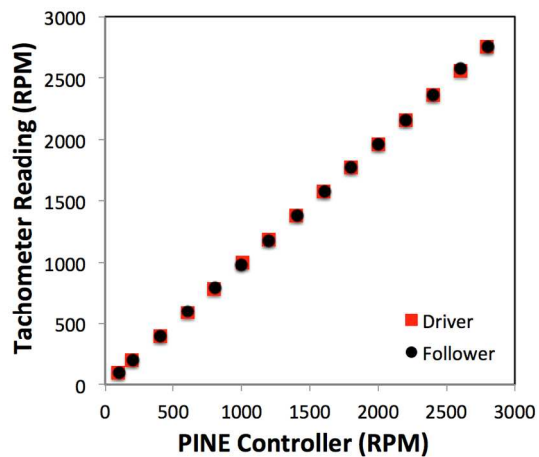


**Figure 2.** The measured rotation speed for both driver (red squares) and follower (black circles) shafts using a tachometer as a function of the applied rotation speed from the Pine controller.

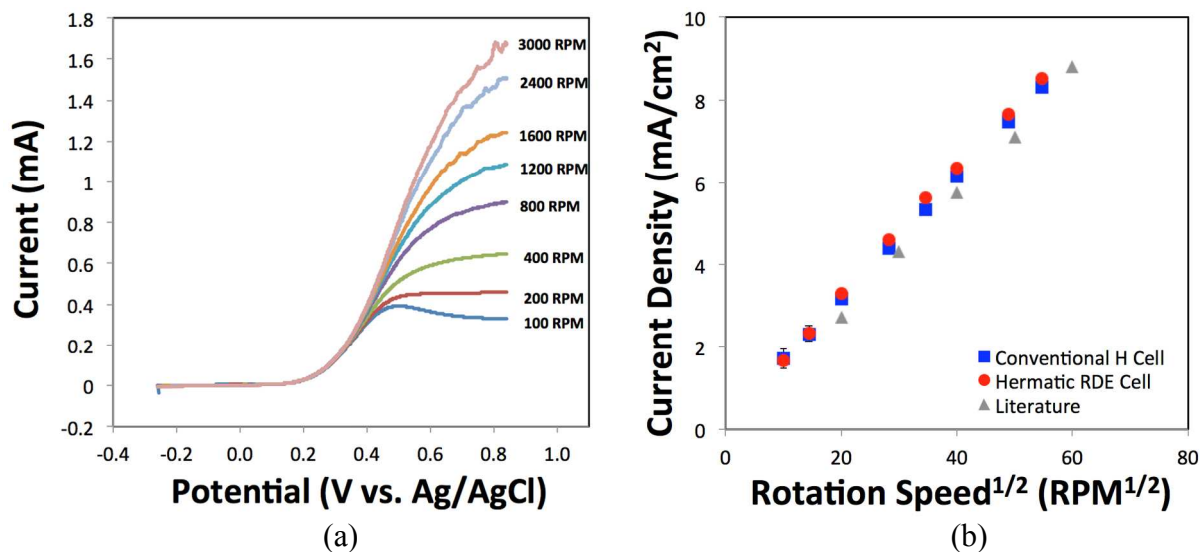


**Figure 3.** (a) Representative rotating disk electrode voltammogram (RDEV) of glassy carbon in 0.1 M  $K_4Fe(CN)_6$  and 0.1 M  $KNO_3$  using the gastight RDE cell. 100 mV/s scan rate. Rotation speeds at 100, 200, 400, 800, 1600, 2400, and 3000 rpm. (b) A Levich plot of the average RDEV current densities at 0.8 V vs Ag/AgCl as a function of the square root of the rotation rate. The measurements from the hermetically-sealed RDE cell are compared to those taken in conventional RDE cells in this report, previously reported values,<sup>21</sup> and the calculated Levich response from Equation 1.



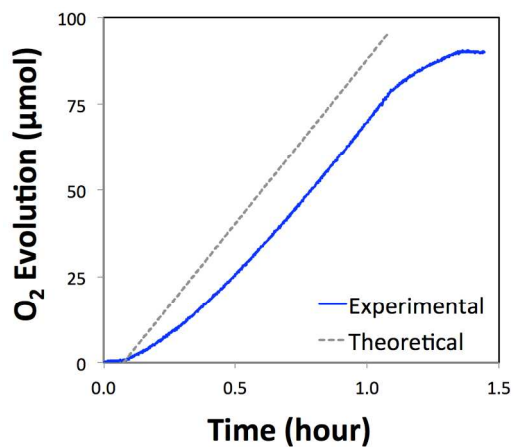
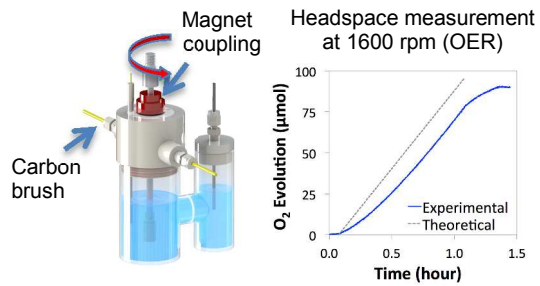


**Figure 4.** An hour-long Faradaic Efficiency (FE) measurement showing the amount of O<sub>2</sub> generated by the alkaline water oxidation reaction of Inconel625 in 1M NaOH. The dashed grey line indicates theoretically predicted values assuming a 100% FE and the solid blue line indicates the actual measured oxygen content in the headspace using the fluorescence O<sub>2</sub> probe. The time-offset between the experimental and theoretical O<sub>2</sub> responses is attributed to the kinetics of the headspace equilibration with the dissolved O<sub>2</sub>. The total amount of headspace O<sub>2</sub> is measured after a ~0.4 h post-electrolysis equilibration time.



Insert Table of Contents artwork here

1  
2  
3  
4  
5  
6  
7  
8  
9  
10  
11  
12  
13  
14  
15  
16  
17  
18  
19  
20  
21  
22  
23  
24  
25  
26  
27  
28  
29  
30  
31  
32  
33  
34  
35  
36  
37  
38  
39  
40  
41  
42  
43  
44  
45  
46  
47  
48  
49  
50  
51  
52  
53  
54  
55  
56  
57  
58  
59  
60